

# Experimental and numerical study on a novel fanless air-to-air solar thermoelectric refrigerator equipped with boosted heat exchanger

Faraz Afshari<sup>\*</sup>, Emre Mandev, Burak Muratçobanoğlu, Ali Fatih Yetim, Mehmet Akif Ceviz

*Department of Mechanical Engineering, Erzurum Technical University, Erzurum, Turkey*

## ARTICLE INFO

**Keywords:**

Thermoelectric  
Coefficient of performance  
Heat exchanger  
Fanless refrigerator  
Renewable energy  
Solar cooling

## ABSTRACT

Peltier cooling systems are generally small, portable and simple in operating principle compared to conventional vapor compression cooling systems. For these reasons, Peltier cooling systems are proposed widely to use in the field. In studies on Peltier coolers presented in the literature, equipment such as pumps and fans is used and this causes noise and vibration. In order to resolve these problems and negative effects, a cooling system was designed and manufactured using completely motionless elements. Additionally, the electricity energy need of this thermoelectric cooling chamber is fully met by solar energy. This study was investigated both experimentally and numerically by using computational fluid dynamics (CFD) methods. By designing a special heat exchanger in the produced air-to-air cooler system, it has been proven that, the Peltier system can work effectively without the need for any elements such as fans. Then the effects of the voltage values applied to the system and the number of Peltier modules have been investigated. The experiments were carried out at 4 different voltage values (1.5, 2.0, 2.5 and 3.0 V) and in 3 different Peltier numbers (1, 3 and 5) in consecutive connections. According to the obtained results, the most suitable situation for reducing the temperature of the cooling chamber were obtained as the voltage was at a maximum of 3 V and the Peltier number was maximum (5 Peltiers mode), where the internal temperature of the cooling chamber decreased to 11.28 °C. It was observed that, the coefficient of performance (COP) values decreased over time in all experiments. Considering the data taken at the beginning of the experiments, the maximum COP value was obtained as 0.04 when 1 Peltier and 1.5 V voltage were applied.

## 1. Introduction

The interest in thermoelectric technology is increasing every passing day due to the developments in technology, the increase in energy demand, efforts to prevent climate change and ensuring that the devices used work with maximum efficiency and minimum energy loss. Although the efficiency of thermoelectric systems used as coolers and generators is relatively lower than conventional systems, it is advantageous of thermoelectric systems as they do not have devices such as compressors, valves, working fluids like refrigerants and etc. The general working principle of thermoelectric coolers is the formation of a temperature difference between two materials because of the voltage applied from the external source [1].

Researchers carry out many studies on thermoelectric cooling systems in different usage areas. For example, in a study Ohara et al. [2] performed a modeling study to determine the optimum geometry as well as the optimum current to power a small thermoelectric vaccine delivery system under World Health Organization requirements. The lowest

temperature of 3.4 °C was reached in the prototype produced. In the test system used, a planar heat pipe was used on the TE hot surface and a fan was placed on the heat pipe. In a study, a thermoelectric (TE) cooling/heating system was proposed for both summer and winter seasons for the vehicle cabin, and 3D simulation was conducted to evaluate the temperature changes in the car cabin during parking [3]. A parametric study was developed using numerical methods to predict the performance of TE generator and cooler. The performance variations were presented and discussed [4]. A novel thermoelectric application in buildings with a comprehensive characterization was carried out. The potential of TEs in buildings was discussed and classification to future research in the field of architecture was done [5]. An experimental study was conducted by Provensi and Barbosa [6] on the effect of using Peltier modules in the air coolers. A counter flow heat exchanger was designed and it was aimed to reveal the thermal behavior of Peltier modules by analyzing the proposed design. The heat sinks were placed on both surfaces of the Peltier modules to reduce the temperature difference between the hot and cold sides. Tian et al. proposed a new type of tube bundle design of tubular Peltier module as an effective technique for air

\* Corresponding author.

E-mail address: [faraz.afshari@erzurum.edu.tr](mailto:faraz.afshari@erzurum.edu.tr) (F. Afshari).

<b>Nomenclature</b>	
$c_p$	Specific heat capacity at constant pressure (J/kg K)
CFD	Computational fluid dynamics
COP	Coefficient of performance
$C_\mu$	Turbulence constant
$I$	Electric current (A)
$K$	Device thermal conductance (W/K)
$m$	Mass (kg)
$P$	Pressure (Pa)
$Q$	Thermal energy (J)
$\dot{Q}$	Heat transfer rate (W)
$T$	Temperature (°C)
$t$	Time (s)
TE	Thermoelectric
TEC	Thermoelectric cooler
$V$	Voltage (V)
$V$	Volume ( $\text{m}^3$ )
$v$	Velocity (m/s)
$W$	Electrical Energy (J)
$R$	Electrical resistance ( $\Omega$ )
$Z$	Figure-of-merit
$\rho$	Density (kg/m)
$\varepsilon$	Turbulent dissipation rate ( $\text{m}^2/\text{s}^3$ )
$\mu$	Dynamic viscosity (kg/m s)
$\mu_t$	Turbulent viscosity (kg/m s)
$\alpha$	Seebeck coefficient (V/K)
<i>Subscripts</i>	
a	Air
c	Cold side
h	Hot side
pe	Peltier
max	Maximum
m	Mean
tot	Total

cooler systems [7].

In another study on the usability of thermoelectric systems in air cooling and heating systems, Peltier modules were placed in the air channel and a water-cooling system was used to remove the heat from these modules. In the experimental analysis, the COP value of the system in the cooling and heating mode were obtained and it was reported that the electric current required to obtain these results is in the range of 4–5 A [8]. In a study on the applicability of thermoelectric in heating and cooling systems of builds, sixteen Peltier modules were utilized. The effect of the temperature difference between the two surfaces of the modules was shown and it was emphasized that the efficiency is more pronounced in the cooling mode. In addition, as a result of the successful tests, it was concluded that a thermoelectric heating-cooling system can be installed in the builds [9]. Exergy analyses of a prototype TE [10], lossless coupling of photovoltaic and TE module through parallel connection [11], investigation on building envelope integrated with TE cooling and radiative sky cooler [12] are the studies in the field, which show the importance of using TE systems in different applications.

It can be mentioned that there is a great interest in determining and developing suitable working conditions of thermoelectric elements used in various application fields. The effects of voltage, flow rates of cooling air and power input on the performance of the TE cooling system in a specific test matrix were investigated by Al-Chlaikhawi et al. [13]. For this purpose, sunflower heat sink with forced convection was added to the hot surface. The COP max value, which was 4.7 at the beginning of the experiments, decreased to 0.13 in a short time. However, in this study, forced convection was created with a fan, and it was stated that the air flow rate was an effective parameter. In a study conducted by Winarta et al. [14], TE performance was tried to be increased by using u-shape heat pipe with heat sink. The U-shape heat pipe was tested by filling methanol at different filling ratios. According to the results of the study, the maximum COP was obtained as 0.03881 and 0.03885 at 45% and 55% filling rates. However, the heat sink was used with a fan. Vian and Astrain [15] aimed to investigate and increase the COP value of the system by producing a thermoelectric cooler prototype. They compared two different systems in which a finned heat sink and a thermosyphon phase changer are utilized to remove the heat from the thermoelectric element. The COP value of the system using the thermosyphon was 32% higher when compared to the other system. Min and Rowe [16] manufactured a thermoelectric cooler prototype and evaluated the COP values of the cooling device. The COP values obtained under the conditions where the internal temperature of the cooler is 5 °C and the ambient temperature is 25 °C were around 0.3–0.5. In addition, the authors emphasized that the COP values of the system can be increased by

improving the heat sinks, thermal interfaces and contact resistances of the modules. Çağlar [17] conducted tests on the thermoelectric refrigerator prototype designed to determine the relationship between the voltage applied to the unite and the thermal performance of the system. The heat sinks and the fans were integrated on both the inside and outside of the Peltier module. COP values of the system were calculated by applying different voltage values to Peltier module and fans. As a result of the data obtained, the optimum voltages to be applied for the Peltier module, inside and outside fans were qualified as 12 V, 3 V and 9 V, respectively. In a study conducted by Martinez et al. [18], the problems encountered in TE refrigerators operating with on/off strategy were studied and it was stated that this strategy increased electricity consumption. In the study, a new idling voltages strategy was proposed and it was revealed that electricity consumption was reduced by 32% and COP increased by 64%. In this study, a 2 W fan was used.

Huang et al. [19] integrated a thermoelectric module into a water-cooling system used for the cooling of electronic devices. From the results of experiments, it was revealed that the efficiency of the Peltier module enhanced with the increase of the electric current, but the high-value electric current also increased the heat production of the Peltier. For this reason, it was emphasized that 7 A electrical current is the optimum value. Moreover, the results showed that integrating Peltier into the water cooling system increases the performance when the heat load is below 57 W. In experiments carried out on a thermoelectric refrigerator manufactured by Gökçek and Şahin [20], a mini-channel water block was used and the waste heat was removed through the thermoelectric element. The internal temperature of the refrigerator was measured by providing water flowing at different flow rates (0.8 and 1.5 L/min). While the COP value of the thermoelectric system was found to be 0.23 in the experiments performed with 1.5 L/min flow rate, it was detected to be 0.19 at 0.8 L/min flow rate.

In the presented studies available in the literature, there are also studies that compare thermoelectric coolers with conventional refrigerators. An important example of this was conducted by Söylemez et al. [21]. In this study, a hybrid refrigerator with vapor compression and thermoelectricity was designed. The designed hybrid refrigerator and vapor compression refrigerator were tested under various conditions and the obtained results were compared. Since the COP values of thermoelectric coolers are lower than the COP values of vapor compression coolers, energy consumption was found to be higher in hybrid refrigerators. The cooling time of the hybrid refrigerator was lower in the range of 30–40% compared to the others. A comparison of single stage and two stage thermoelectric coolers was made by Gao et al. [22]. It was demonstrated that the two-stage thermoelectric system

reached lower temperature values and maintained the coldness for a longer period of time. Hermes and Barbosa [23] designed and tested different types of coolers including stirling, thermoelectric and vapor compression. The experiments were carried out at two different ambient temperatures and it was stated that the stirling and vapor compression coolers showed similar thermal performance, but the performance of the thermoelectric cooler was lower than the others, and that the efficiency of the system can be increased by making serious modifications. In the experiments, COP analysis was performed for all systems and the COP value of the thermoelectric cooler was the lowest value with 0.2.

An important evaluation criterion for thermoelectric coolers is the temperature drop in the chamber. Lee et al. [24] has presented an exemplary study on this subject. They designed a thermoelectric refrigerator and investigated this issue both numerically and experimentally. In the experiments using two-phase thermosiphon, it was stated that while the ambient temperature was about 25 °C, the internal temperature of the refrigerator was –4.6 °C on average. In a study conducted by Yadav et al. [25], a cooler with a fan on the cold surface and a hot surface in direct contact with the ambient air was designed and tests were carried out on it. According to the results of the study, a temperature decrease of 10–12 °C was observed in the test room within about 10 min. In a study on the subject, a numerical model was proposed to predict the internal temperature of the Peltier cooler by Astrain et al. [26]. This proposed numerical model was compared with the experiments on the designed and produced a prototype, and the maximum error in the COP value was detected as ±7%. In a review study conducted by Riffat and Ma [27], improving the COP values of thermoelectric cooling systems was discussed. As a result of this comprehensive examination, the researchers obviously demonstrated the effect of thermoelement sizes on the COP values of thermoelectric devices. It was reported that thermoelectric modules with large thermoelements should have a higher COP values.

As a result of a detailed literature review, it is seen that for TE coolers, forced convection applications are mainly used on both sides of the TE modules. Studies in which both sides or only one side are exposed to heat transfer by natural convection are limited. A few examples of these were given below. An investigation was performed on a prototype thermoelectric refrigerator by Martinez et al. [28]. In the prototype built, finned heat sinks were placed on both sides of the thermoelectric module and it was considered to work under natural convection conditions from the inside of the refrigerator. In this study, a computational model was proposed and compared with the experimental data. It was noted that the proposed model accords quite well with the actual results. Posobkiewicz and Górecki [29] designed a thermoelectric system that can be used for cooling electronic devices and integrated a heat sink and fan into this system. The effect of the fan in terms of the cooling performance of the system was examined and observations were carried out under forced convection and natural convection conditions. A decrease of 4 °C was observed in the temperature of the resistor, which is intended to be cooled under natural convection conditions. When a fan with 6 V voltage is utilized, this value rose up to 16 °C. In the numerical study carried out on the thermoelectric module, a heat sink was placed on the module and its performance under natural convection conditions was investigated. The fins of the heat sink were devised to be conical and narrowed from the base to the tip [30]. In another study, useful methods were used to remove the heat from the thermoelectric module to the ambient and, natural convection and forced convection were discussed. It was determined that the size of the heat sink used for natural convection should be 4 times larger than the other in order to have the same effect of natural convection and forced convection from the compared heat transfer methods [31]. In a research, the performance of the thermoelectric system was examined and the COP value was calculated. A fin heat sink was placed on the cold side of the Peltier module and natural convection heat transfer was ensured. The maximum COP value of the system was detected as 0.31 when 5 V voltage was applied [32]. In the study carried out by Jugsujinda et al. [33] a TE cooler with 40 W

electrical power was produced. In this study, while a fan was not used on the cold surface, it was used on the hot surface. Researchers examining the change of temperature in the test room with time focused on the temperature increase rate, temperature difference and time. In the study conducted by Rahman et al. [34], various experiments were carried out by meeting the electrical energy needed by the TE cooler with solar applications. However, in the study, a proposed heating load was met by using a fan with a capacity of 3.846 W.

The vast majority of the studies outlined above used external devices such as a fan or pump. Although this increases the performance, it increases the complexity of the system and reduces the silent operation potential, which is one of the most important advantages of TE systems. Additionally, studies in the literature meet the electrical energy needed by TE systems from the network. This design reduces the mobility of coolers. In this study, the potential to increase the performance of the system without the need for an external device was evaluated by using a new heat exchanger. Moreover, it has been shown that the usability potential can be increased by providing the energy needed by the system with solar energy. With these two fundamental changes, the system has been manufactured in a completely original form. In particular, a suitable heat exchanger has been designed for each of the hot and cold surfaces of the TE. In this context, an attempt has been made to resolve the gap in the literature related to the application of natural convection in thermoelectric systems. Both experimental and numerical methods have been used to evaluate the system performance and the effects of the TEs arrangement and electrical power on the temperature reduction and COP value.

## 2. Methodology

### 2.1. Experimental procedure details

It is known that the cooling load and COP value of thermoelectric cooling systems are significantly affected by the Peltier arrangement, number and the applied voltage. However, this effect is strongly related to the geometry of the heat exchangers and the cooling chamber. In this research, a styrofoam-made cooling chamber with the capacity of 23 × 28 × 37 cm was used to analyze the effects of applied voltages (1.5, 2.0, 2.5 and 3.0 V) and Peltier number on the performance of a thermoelectric cooler (TEC) system. The experiments were made on an air-to-air TE by installing 1, 3 and 5 Peltier configurations. Heat exchangers are significant elements in heating and cooling devices [35–37], which should be installed in TE systems to transfer heat from the source to the designated destination. On both cold and hot sides of the Peltier module, suitable heat exchangers were designed and located to increase heat transfer in the cooling system.

Extended surface application, which is one of the passive methods commonly used in heat transfer enhancement, was preferred in the design of heat exchangers. In thermoelectric cooling applications, fans are used for air circulation to obtain efficient heat transfer in the heat exchangers. The usage of fans causes both noise in the system and an additional energy requirement. In this design, the fans are removed from the system by employing novel heat exchangers with the extended surfaces. The heat transfer mechanism around the internal and external heat exchangers has been changed from forced convection conditions to natural convection conditions. Although relatively low convection coefficients under natural convection conditions are expected, effective cooling has been aimed by increasing the heat transfer area with extended surfaces. The energy consumption of the system due to the fan has been reduced. In addition, in the installed setup, it has been thought that the refrigerator will work silently and in fanless conditions. A specially designed aluminum bar heat exchanger is used inside the cooling chamber and in the aluminum plates were used to boost the performance of the outer heat exchanger. The base dimensions of the internal heat exchanger are 4 × 4 cm and the bar diameter and lengths are 0.3 and 19 cm, respectively. The dimensions of the outer plates are 5

$\times 20$  cm and are designed to be very thin. In order to enhance the heat transfer between connecting surfaces of the Peltier and heat exchangers, HY510 thermal paste with high thermal conductivity has been used. Generally used Peltier dimensions are 40x40x4 mm. In the same way, Vicko brand TEC1-12715 model Peltier modules were used in this work. During the experiments, heat transfer characteristics of the Peltier cooling system were investigated employing a high-quality TESTO 885-2 thermal imager. The measuring range of the thermal imager is between  $-30$  °C and  $+350$  °C, with accuracy and thermal sensitivity of  $\pm 2$  °C and  $<30$  mK at  $30$  °C, respectively. In the experiments, 4 thermocouples were used inside the cooling chamber and the temperature values were taken during the test (3500 s) and the obtained values were transferred to a computer by means of a datalogger. The average of the

obtained temperatures was taken and the calculations were made on the average values.

The required power for the used TE elements operating in different modes was powered by a solar system. The solar system includes 24 units of 1.5 W Star Solar brand CNC85X115-18 model 85  $\times$  115 mm photovoltaic cells. The solar cells were connected to the Mestech brand 20A-12/24V solar charge controller. SA-TEK brand 12N6.5L-BS model gel battery was used for charging. In the solar power system, the current and voltage values were controlled by using Micron brand Xl4016 model 300 W DC Buck Converter between the gel battery and the TE elements. In Fig. 1 schematic view of the entire system powered by solar panels and arrangement of 1, 3 and 5 Peltiers modes are given (In the Figure, the solar panel has been placed near the whole cooling system to display

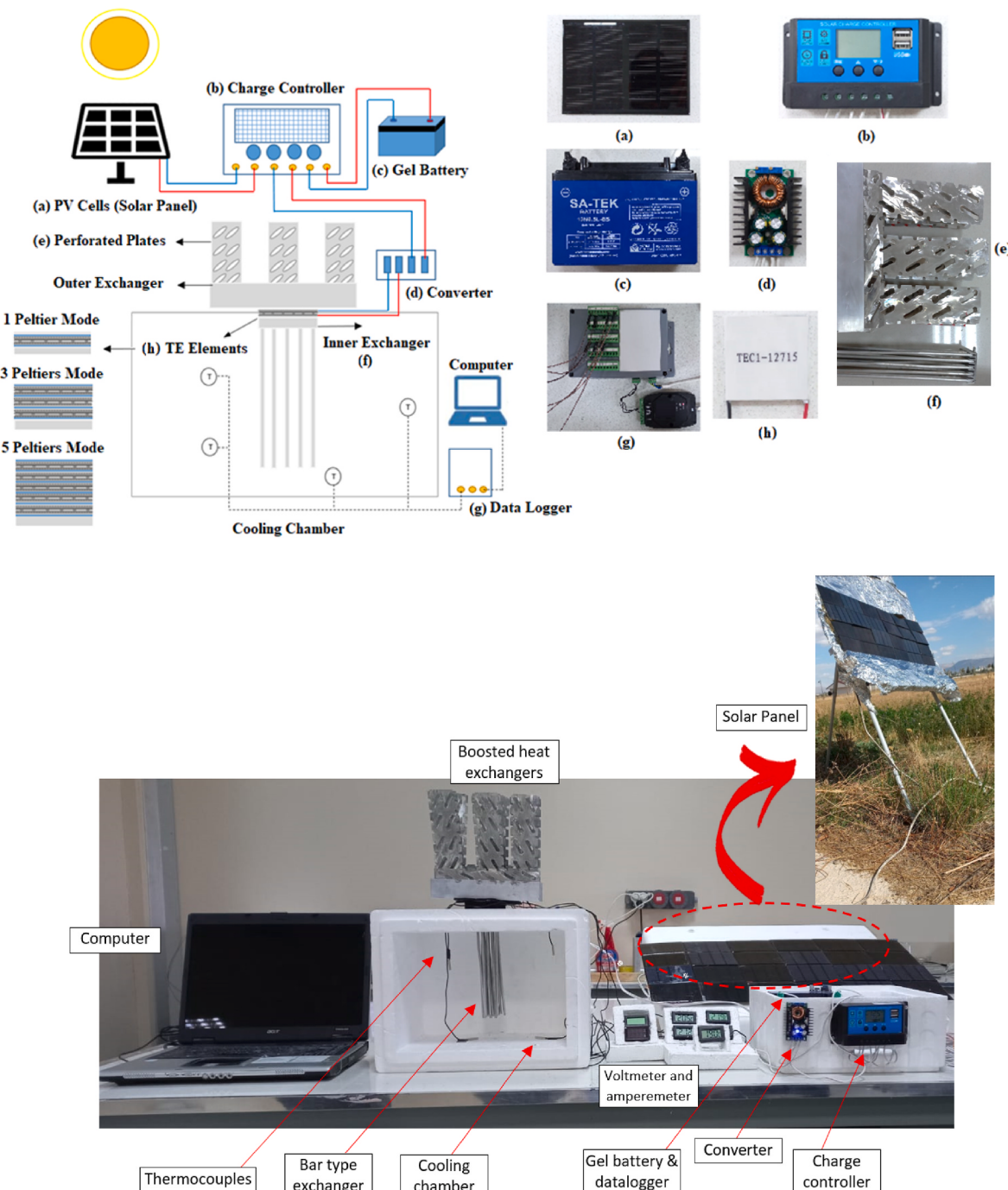


**Fig. 1.** Schematic view of the fanless cooling system and arrangement of 1, 3 and 5 Peltiers modes and a picture of experimental setup.

all elements in one image. During experiments, the solar panel was located outside exposed to direct solar radiation). The time dependent power curves of the photovoltaic cells used for battery charging in the Erzurum city center in Turkey are also presented in Fig. 2 for two different days (Erzurum city is located in the Eastern Anatolia Region on 39° 55' 23" North latitude and 41° 10' 12" East longitude).

It should be stated that, before starting the analysis, heat transfer and XRD (X-ray diffractometer) experiments were performed for copper and aluminum heat exchangers for the selection of heat exchanger material. The XRD analyses of samples were performed by using an X-ray diffractometer (GNR-Explorer XRD). During XRD characterization, the XRD device was operated at 40 kV and 30 mA with Cu-K $\alpha$  cathode with a  $\lambda = 1.540 \text{ \AA}$  wavelength. The chemical compositions of the phases formed were obtained by matching with the International Center for Diffraction Data (ICDD) standard cards. XRD patterns of Copper and Aluminum samples are shown in Fig. 3. It was seen that copper samples completely exhibited Cu peaks and pure aluminum peaks were diffracted from the aluminum material. While the dominant phase for Cu material was the peaks diffracted from the (202) plane, it was (200) for aluminum materials. The aluminum material was chosen for heat exchangers related to heat transfer and XRD experiments.

## 2.2. Numerical approach

CFD simulation of the numerical approach has been performed by modeling the problem and using novel heat exchangers in the Peltier cooling system to analyze cooling performance of the designed refrigerators. The under evaluation Peltier cooling system thermodynamically was optimized and the COP value of the system was obtained under different operating conditions. The model of the cooling chamber and heat exchangers were simulated exactly according to the experimental setup in the same dimensions. ANSYS Fluent 2021 software was employed to simulate the model and all processes including drawing of geometries, mesh creation, definition of boundary conditions and solution were carried out using this CFD software.

The problem was assumed to be steady state. The cooling chamber was insulated and its walls were closed to heat transfer. In Fig. 4, the mesh qualities of different parts of the cooling chamber and external boosted heat exchanger, have been presented. In the mesh creation process, the produced mesh configuration has been considered carefully to have the required mesh quality. Near the walls and areas near the boundaries more compact and finer meshes were applied. Mesh numbers of 2,200,000 and 3,400,000 were generated for the cooling chamber and external exchanger, respectively. In this section curvature mode mesh production with a growth rate of 1.2 has been performed. In this work,

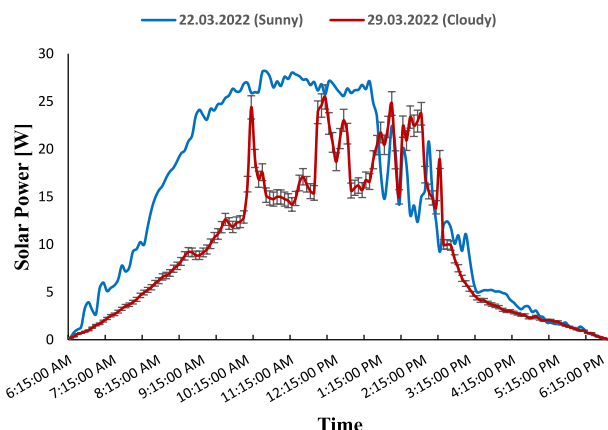


Fig. 2. The time dependent power curves of the photovoltaic cells for two different days.

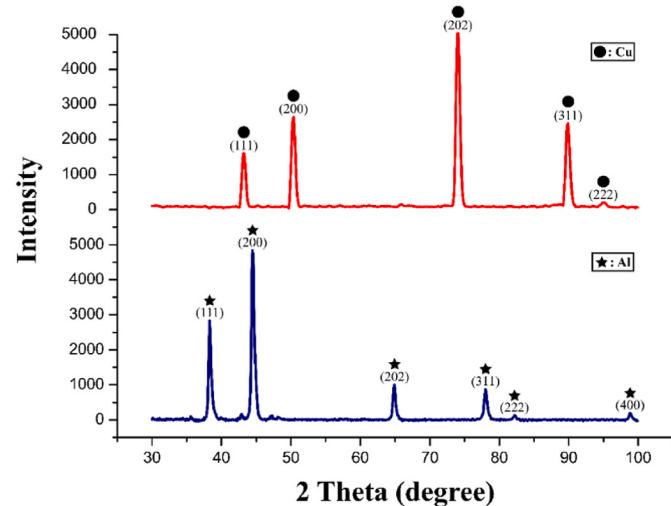


Fig. 3. XRD patterns of Copper and Aluminum samples.

average and maximum skewness values for the inner and outer domains were 0.22, 0.83 (cooling chamber) and 0.24, 0.96 (outer boosted heat exchanger), respectively. In order to achieve the required accuracy, suitable mesh generation with appropriate mesh elements was considered. In this regard in Fig. 5, grid independence analysis has been provided for the cooling chamber temperature and the surface temperature of the heat exchanger.

The double precision solution does run slower and takes up more memory but is more accurate and so double precision solution was selected. Solvent type was defined as pressure-based and the standard k-epsilon model was chosen. In the CFD solution, the inside of the cooling chamber was defined as the solution domain and its walls were assumed to be insulated. The aluminum material presented in the Fluent database was chosen as the materials of the inner exchanger bars and external exchanger. From the experiments, the temperature of the heat exchanger inside the cooling chamber was determined to be approximately 278 K. For this reason, a constant temperature value of 278 K was applied to the base of the bar type heat exchanger in the model as the boundary condition in the numerical solution. The bars (aluminum rods) and all the walls of the cooling chamber are defined as Walls. Gravity acceleration value of 9.81 m/s<sup>2</sup> was defined and the air was assumed to be an ideal gas. As the initial boundary condition, the temperature of all surfaces of the system and the air inside was defined to be 293 K (room temperature). In solution methods, Couple scheme was selected in order to get more precise results. Discretization is one of the most important parts of CFD methods. At this stage, the chosen method for momentum, energy and density was the second order upwind and also for turbulent kinetic energy and turbulent dissipation rate first order upwind were selected. It was observed that solution of model is converged after 200 iterations.

## 2.3. Analysis and calculations

COP value of all heating and cooling devices represents the total efficiency and is defined as one of the most significant part of analyses. By referring to the literature, it can be found that, in scientific articles on thermoelectric refrigerators, calculations are performed in two different ways. In the first model, calculations start with the prediction of the thermoelectric heating and cooling rate. By assuming constant electrical and thermal properties of TE, heat transfer amounts at cold and hot sides ( $Q_c$  and  $Q_h$ ) are given as [38–40],

$$\dot{Q}_c = \alpha T_c I - \frac{1}{2} (I^2 R) - K(T_h - T_c) \quad (1)$$

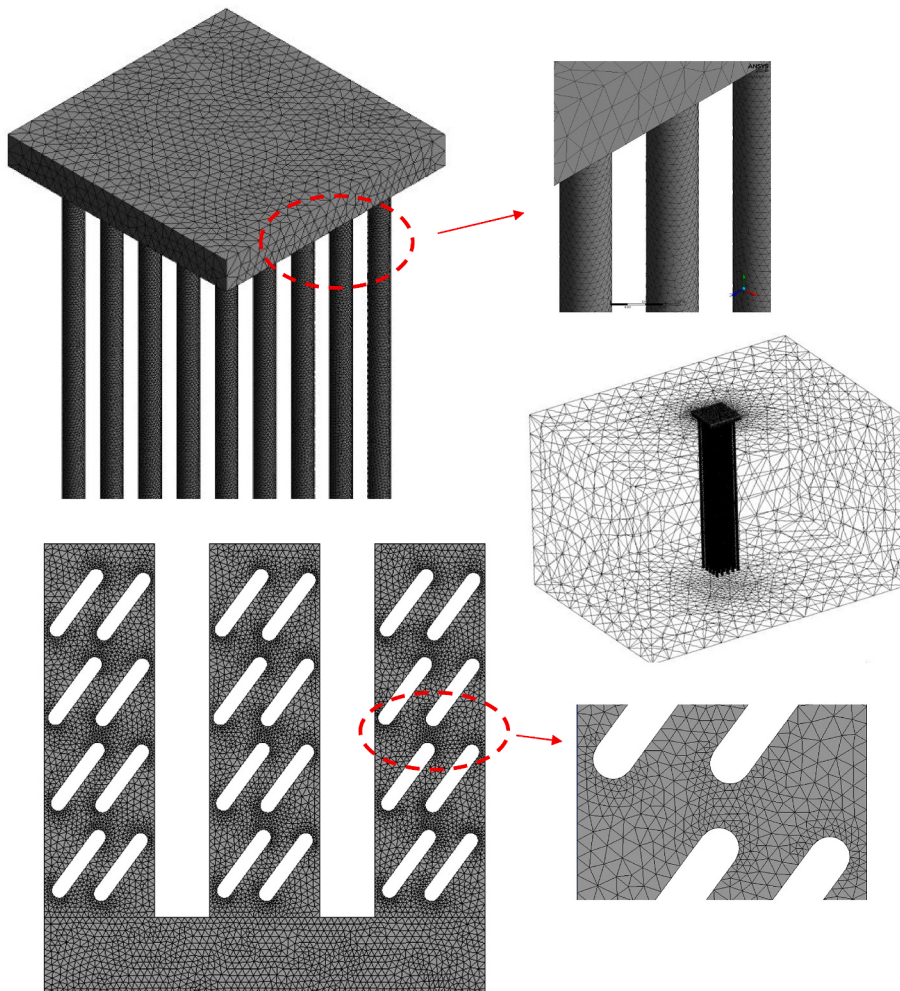


**Fig. 4.** Mesh configuration of cooling system and boosted heat exchangers.

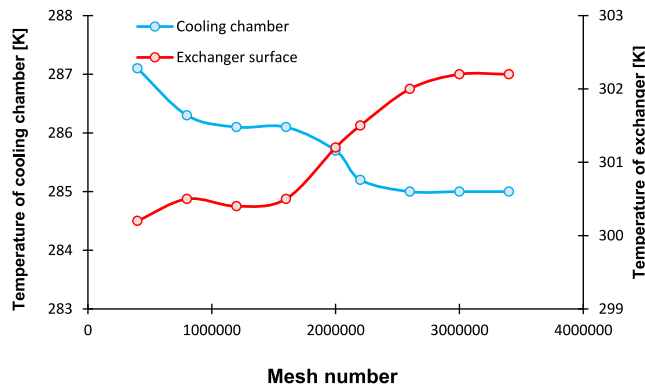


**Fig. 5.** Mesh analysis using obtained data from temperature of cooling chamber and external heat exchanger.

$$\dot{Q}_h = \alpha T_h I - \frac{1}{2} (I^2 R) - K(T_h - T_c) \quad (2)$$

Thermoelectric cooler COP can be calculated as,

$$COP_{c,max} = \frac{T_c}{T_h - T_c} \frac{\sqrt{1 + ZT_m} - \frac{T_h}{T_c}}{\sqrt{1 + ZT_m} + 1} \quad (3)$$

here  $ZT_m$  is the TE material figure-of-merit at average cold and hot side.

In the second method that was used in this present study, thermodynamic method is utilized and power consumption of the Peltier module, is taken into consideration and so the total COP value of the cooling system can be found as,

$$COP_{tot} = \frac{Q_c}{W_{pe}} \quad (4)$$

In this equation, the total amount of COP can be obtained by dividing heat ( $Q_c$ ) transferred from the cooling chamber of refrigerator by total power consumed. In this equation, the electrical power consumed by Peltier module is calculated by following equation,

$$W_{pe} = VI \times t \quad (5)$$

In this equation,  $V$  and  $I$  are the applied voltage and electrical current values used by Peltier module. Air mass inside the cooling chamber should be calculated to evaluate heat transferred from the cooling chamber. Having the volume of the chamber and air density we have,

$$m_a = \rho_a V_a \quad (6)$$

The heat transferred from the cooling chamber to the environment is expressed as,

$$Q_c = m_a c_{p,a} [T_{2,a} - T_{1,a}] \quad (7)$$

In Equation (7),  $T_{1,a}$  and  $T_{2,a}$  are the first and last mean temperatures of the cooling chamber over test time and  $m$  is the air mass inside (obtained in Equation (6)). It should be noted that, temperature of the cooling chamber was obtained using placed thermocouples inside

cooling chamber and the mean temperature was calculated to use in analyses.

Momentum, continuity and energy equations are the main governing equations in CFD simulation and solution of the problem, which are presented respectively in following equations,

Momentum equation is given as,

$$\nabla \cdot (\rho \vec{v} \cdot \vec{v}) = -\nabla P + \nabla \cdot \left( \mu \left[ (\nabla \vec{v} + \nabla \vec{v}^T) - \frac{2}{3} \nabla \cdot \vec{v} I \right] \right) \quad (8)$$

Continuity equation can be expressed as,

$$\nabla \cdot (\rho \vec{v}) = 0 \quad (9)$$

Energy conservation balance is given as,

$$\nabla \cdot (\vec{V} (\rho E + P)) = \nabla \cdot k_{eff} \nabla T - h \vec{J} + \left( \mu \left[ (\nabla \vec{v} + \nabla \vec{v}^T) - \frac{2}{3} \nabla \cdot \vec{v} I \right] \vec{v} \right) \quad (10)$$

k- $\epsilon$  model is an extensively used model in the CFD approach, which is used in this study to simulate the present problem. In k- $\epsilon$ model, two transport equations have been provided as a general definition for turbulent flow. These two equations are defined as turbulent kinetic energy and rate of dissipation of kinetic energy ( $\epsilon$ ).

k- $\epsilon$  equations are expressed as [41,42],

$$\frac{\partial}{\partial x_i} \left( \left( \frac{\mu_t}{\sigma_k} + \mu \right) \frac{\partial k}{\partial x_j} \right) - (\rho \epsilon) + G_k = \frac{\partial}{\partial x_i} [(u_i \rho k)] \quad (11)$$

$$\frac{\partial}{\partial x_i} (u_i \rho \epsilon) = \frac{\partial}{\partial x_j} \left[ \left( \frac{\mu_t}{\sigma_\epsilon} + \mu \right) \frac{\partial \epsilon}{\partial x_j} \right] + \left( \frac{\epsilon}{k} G_k C_{1\epsilon} \right) - \left( \rho \frac{\epsilon^2}{k} C_{2\epsilon} \right) \quad (12)$$

$$G_k = - \frac{\partial u_j}{\partial x_i} \overline{\rho u'_j u'_i} \quad (13)$$

$$\mu_t = \rho C_\mu \frac{k^2}{\epsilon} \quad (14)$$

Generally, various parameters such as instrument selection, calibration, observation, scheduling, reading, and sometimes environmental parameters cause calculation errors and therefore the amount of error rate should be considered. Uncertainty analysis for experimentally measured values is given in the form of mathematical relationships. Generally, if the output quantity  $\beta$  is assumed to be calculated from input values  $\alpha_1, \alpha_2, \dots, \alpha_n$  according to a function as  $\beta = F(\alpha_1, \alpha_2, \dots, \alpha_n)$ , the combined uncertainty of the output quantity  $U_c(\beta)$  can be obtained by uncertainties of the input data  $u(\alpha_i)$  as follows [43],

$$U_c(\beta) = \sqrt{\left[ \frac{\partial \beta}{\partial \alpha_1} u(\alpha_1) \right]^2 + \left[ \frac{\partial \beta}{\partial \alpha_2} u(\alpha_2) \right]^2 + \dots + \left[ \frac{\partial \beta}{\partial \alpha_n} u(\alpha_n) \right]^2} \quad (15)$$

From the given equations, the COP of TEC is a function of energy consumed by the Peltier module and the cooling rate of the system. So the uncertainty of the cooling setup is computed by equation (16), from which the calculated uncertainty for COP was  $\pm 2.9\%$ .

$$U_c(COP) = \sqrt{\left( U_I \frac{\partial COP}{\partial T_{cooling\ chamber}} \right)^2 + \left( U_W \frac{\partial COP}{\partial \dot{W}} \right)^2} \quad (16)$$

### 3. Results and discussion

In this section, the experimental and numerical results are presented and discussed and the temperature variations of cooling chambers, the coefficient of performance and cooling loads ( $Q_c$ ) are evaluated on diagrams and contours. By using the ANSYS-Fluent 2021 package program, CFD simulation results are also given as temperature and velocity contours.

### 3.1. Experimental results

In this study, experiments were performed under different operating conditions by optimizing the applied voltage and thermoelectric states as 1, 3 and 5 Peltier modes.

The temperature drop inside the cooling chamber was recorded during the test time and the applied electrical power value and the coefficient of performance were calculated and compared. At first, the temperature drops inside the cooling chamber are presented in Fig. 6a, b and c for 1 Peltier mode, 3 Peltiers mode and 5 Peltiers mode respectively. Moreover, the results for applied voltages of 1.5, 2, 2.5 and 3 V can be compared in the figures. Given the temperature results in Fig. 6, a lower temperature is obtained using more Peltier numbers. From the figures it can be concluded that a more effective temperature drop is obtained for the 5 Peltiers modes when the applied voltage is 3 V (Fig. 6c). The reason for this issue is that the internal energy inside the

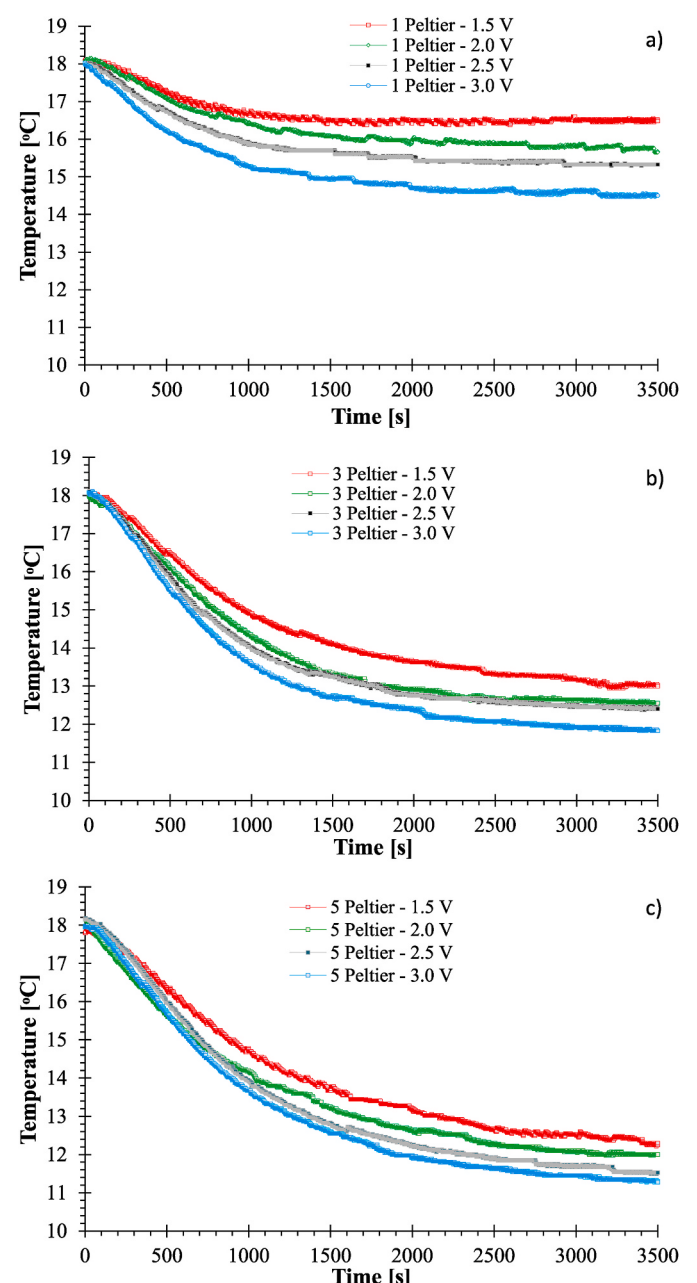


Fig. 6. Temperature variation with test time for a) 1 Peltier mode b) 3 Peltiers mode c) 5 Peltiers mode at different applied voltages.

box can be drawn faster by supplying more electrical energy. This situation has been proven by many studies in the literature [44–46]. By applying the voltage value of 3 V, the temperature reduction was calculated as approximately  $\Delta T = 3.5^\circ\text{C}$  for the 1 Peltier mode,  $\Delta T = 6.2^\circ\text{C}$  for 3 Peltiers modes and  $\Delta T = 6.7^\circ\text{C}$  for 5 Peltiers modes.

In the study by Dongare et al. [47], it was stated that a more effective cooling can be achieved by increasing the Peltier number. The proposed situation in this study was also proven experimentally. For having a better comparison, temperature variations for 1, 3 and 5 Peltiers modes have been presented at 3.0 V (Fig. 7). According to the results obtained in this figure, the temperature drops in the 1 Peltier mode appeared to be quite small. When the Peltier number increases to 3, a big difference has emerged and a better performance has been obtained in terms of temperature reduction. In the figure, if the Peltier number is taken as 5, the lowest temperatures have been reached according to the experiments obtained. Another issue is that while the temperature curve decreases more rapidly in the first seconds, it is approximately fixed toward the end.

In Fig. 8, temperature variations of the surface of the outer boosted heat exchanger have been presented during test time for 3 Peltiers mode. The obtained results for different voltages showed that by increasing applied voltage temperature of outer exchanger increases. In Fig. 9, temperature variations of the surface of external heat exchanger have been presented during test time for 1, 3 and 5 Peltier modes at 3 V. As expected, the surface temperatures of the external heat exchanger increased with the increase of the Peltier number. In addition, in the 5 Peltiers mode, it took about 2500 s for the surface temperatures to reach equilibrium, while in the 1 Peltier mode this time was around 1000 s.

In Fig. 10, COP variations during test time for 1, 3 and 5 Peltier modes are given at different voltages. Generally, it is known that the COP value decreases with time and approaches 0 for all Peltier arrays and all voltage values [48–50]. With the decrease in the temperature of the cooling chamber, the amount of energy that can be drawn from the chamber also decreases. This is the reason for the decrease observed in the COP over time. The highest COP value was reached at 1.5 V.

In Fig. 11, the total  $Q_c$  value (amount of heat energy drawn from the cooling chamber) over test time is presented. Columns demonstrated in dark colors at the right side of the histogram belong to the 5 Peltier modes. It is seen that the total thermal energy taken from the cooling chamber by using 5 Peltiers is greater than that of the 1 and 3 Peltiers. In addition, by increasing the applied voltage,  $Q_c$  value increases gradually in all experiments. The minimum  $Q_c$  value was obtained as 25.6 J for 1 Peltier mode at 1.5 V and maximum was obtained as 106.6 J for 5 Peltiers mode at 3 V.

In Fig. 12, the average COP diagram calculated by considering instantaneous COP values during test time is presented. In this regard, the COP values within 3500 s were obtained for all Peltier modes at

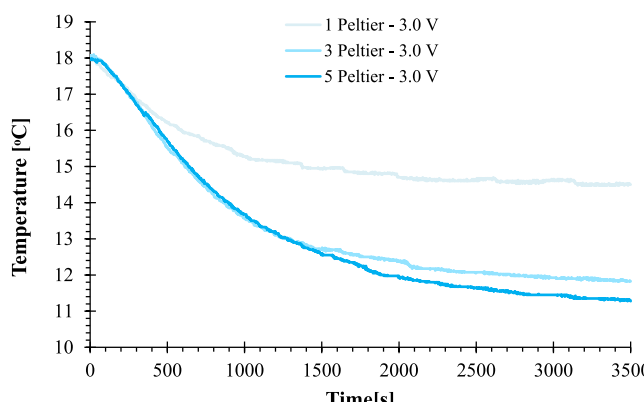


Fig. 7. Temperature variation with test time for 1, 3 and 5 Peltier modes at 3.0 V.

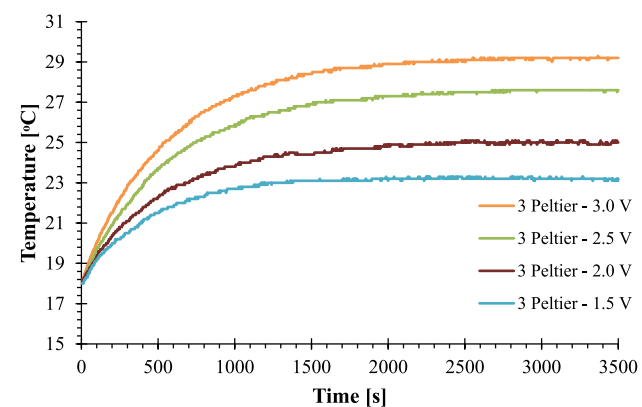


Fig. 8. Temperature variations of the surface of the outer heat exchanger during test time for 3 Peltiers mode at different voltages.

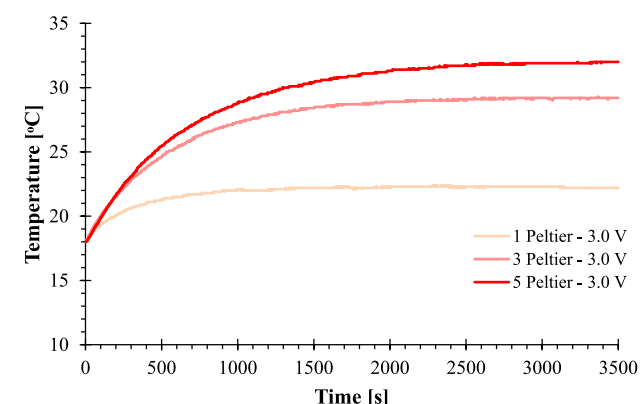


Fig. 9. Temperature variations of the surface of outer heat exchanger during test time for 1, 3 and 5 Peltier mode at 3 V.

different voltages. This figure is provided to evaluate the total COP value during test time. According to the results attained it can be seen that, the COP average of the 1 Peltier mode at applied voltage of 1.5 V is in maximum level, where its value is about 0.0103. The minimum average COP was also obtained for the operating modes with 5 Peltiers at the voltage of 3 V. By comparing all obtained results, it can be stated that if the applied voltage is lower, average COP of the system will be higher. By reviewing the studies presented in the literature, it can be seen that these data are supported by several studies [51,52].

### 3.2. Thermal image analysis results

The temperature variations of the cooling system were measured in the laboratory conditions by using a thermal imager in such a way that the temperature distribution in the cooling chamber, inner aluminum bars of heat exchanger and boosted outer exchanger can be evaluated. In Fig. 13, the obtained image by thermal camera is given where the system was operated using 5 Peltiers with voltage applied as 3 V. When the achieved figure is examined, it is observed that the warmest region is the boosted outer heat exchanger. Here, how natural convection heat transfer takes place is also seen. The temperature distribution inside the refrigerator is not homogeneous and the areas close to the aluminum bars are the coldest regions. In Fig. 14 temperature variation on the vertical direction has been demonstrated for the lines P1 indicated on Fig. 14 left side. In addition, this data was used to validate the numerical results discussed in detail in the next section.

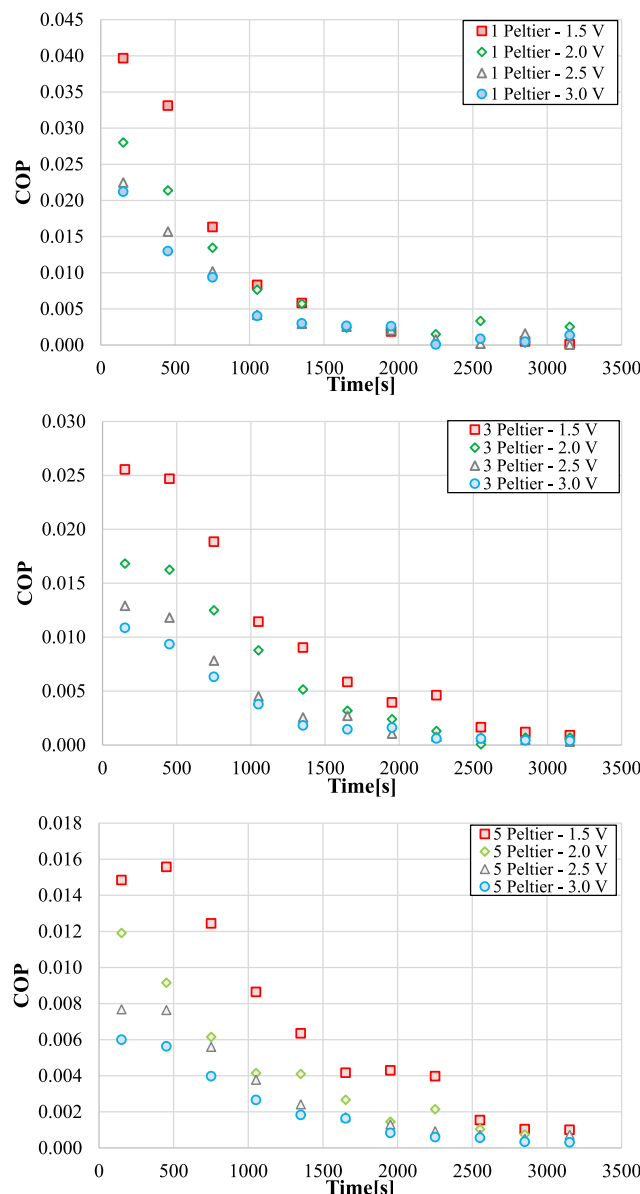


Fig. 10. COP variations during test time for (a) 1, (b) 3 and (c) 5 Peltiers modes at different voltages.

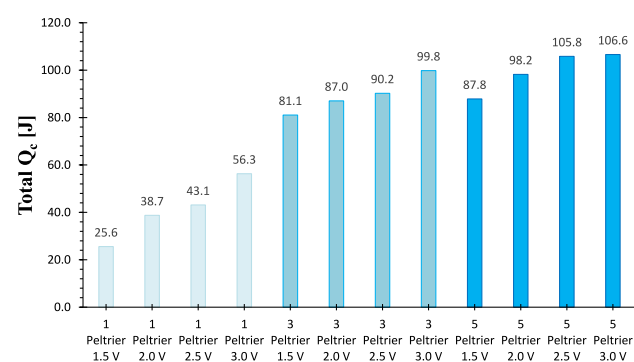


Fig. 11. Total Cooling Load ( $Q_c$ ) for 1, 3 and 5 Peltiers modes at different voltages (1.5, 2.0, 2.5 and 3.0 V).

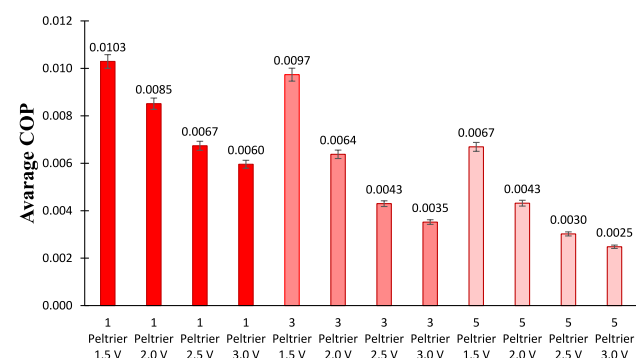


Fig. 12. Average COP for 1, 3 and 5 Peltiers modes at different voltages (1.5, 2.0, 2.5 and 3.0 V).

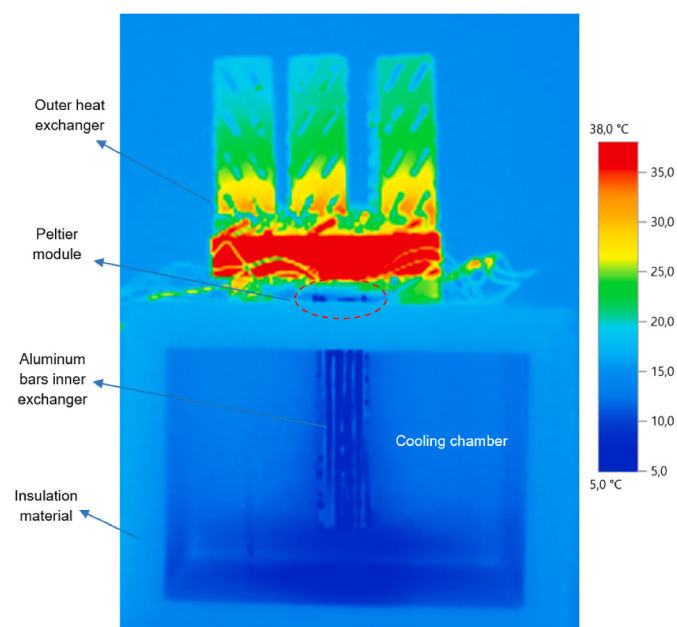
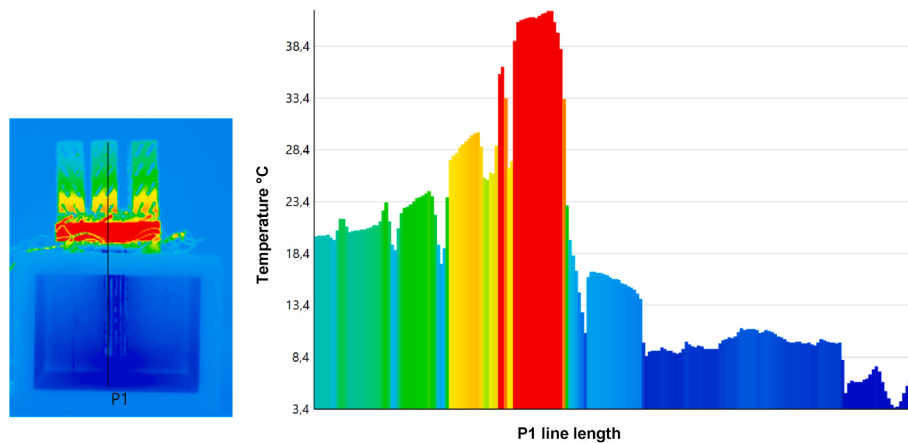


Fig. 13. Temperature distribution inside cooling chamber and outer heat exchanger at 5 Peltier mode and 3V.

### 3.3. Numerical results

Numerical studies have become an integral part of research in the literature, and researchers survey main parameters such as temperature distribution and flow structure in energy systems by using CFD simulation methods [53–55]. In this section, obtained results from CFD solutions have been presented in the form of contours and diagrams. Initially, the CFD results of the external heat exchanger have been analyzed. In Fig. 15, temperature distribution around external heat exchanger and fins are given. It can be seen that the base section of the exchanger is the warmest area in the defined domain. The temperature of the perforated plates decreases with distance from the base. In the upper part of the boosted heat exchanger, the heating of the air and transmission of thermal energy to air by natural convection can be observed.

In Fig. 16, streamline results of air ambient around external heat exchanger have been illustrated. Flow structure shows that by increasing the air temperature in lower sections, an air movement has happened in which direction is from bottom to top, and the vortex flow is formed in the upper sections. Additionally, the natural convection heat transfer is more effective at the top of the center and the velocity of the air is higher. The maximum velocity value was found to be  $2.5 \times 10^{-1}$  m/s.



**Fig. 14.** Temperature variation on line P1 recorded by thermal imager.

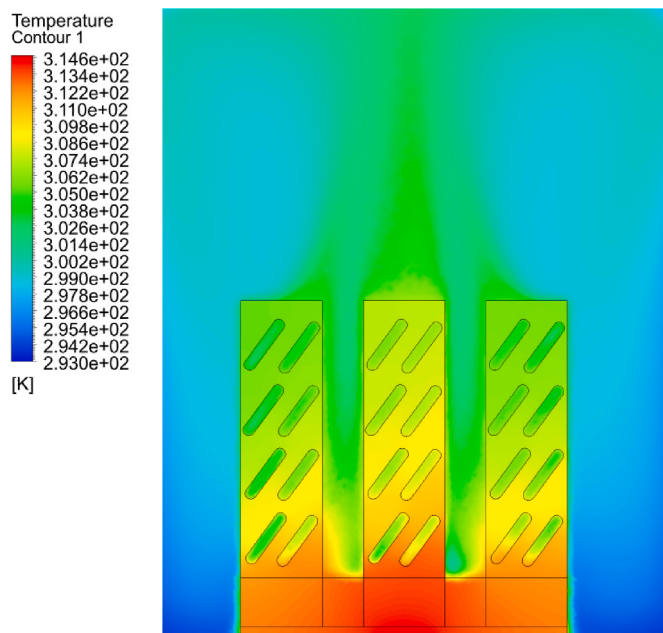


**Fig. 15.** Temperature distribution around the external heat exchanger.

Fluid flow and temperature distribution are evaluated in more detail in 3D volume rendering contours, and it is useful to observe the whole volume of the system to have a better analysis. The mentioned condition is not easy to detect visually in the experimental study and CFD simulation can reveal behavior of fluid and temperature distribution, which is one of the important advantages of CFD. The velocity and temperature volume rendering results of cooling chamber are given in Fig. 17. Due to the higher density of the cold air, it is clearly seen that there is a downward movement and the hot air is collected in the upper parts of the cooling chamber.

Fig. 18 shows the streamlines and velocity vector results of cooling chamber. From the streamline results, the formation of vortexes with the cooling of the air inside can be clearly seen, which has been appeared around the aluminum rods. These vortexes formed are the result of the changes in the density of the air cooled by natural convection and its downward movement. These contours have demonstrated the effect of the natural convection mechanism that is the main purpose of the experiments in this study. The maximum velocity value obtained was  $2.2 \times 10^{-2}$  m/s as seen in the vector and streamline results. The reason why this value is lower than the velocity value in Fig. 16, is that the thermal energy is higher in the upper part (boosted heat exchanger) and the

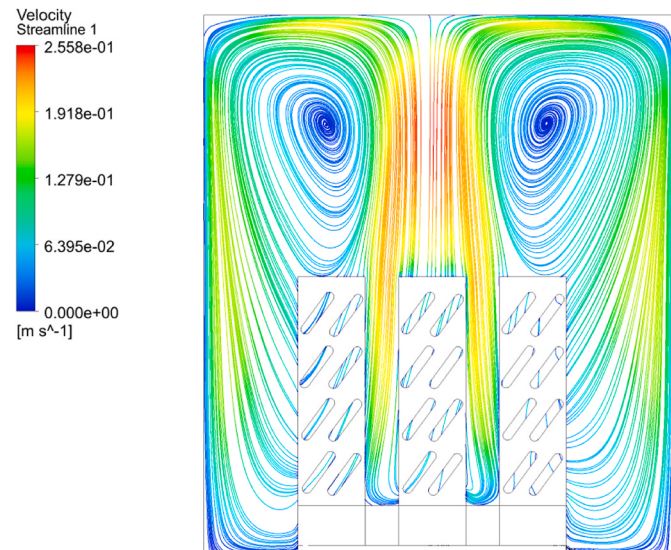


**Fig. 16.** Streamline results of air ambient around external heat exchanger.

temperature difference between the air and the surface is large. Considering the size and density of the vectors, it is seen that there is more intense and high-speed air movement near the rods and at the downside of the cooling chamber.

Temperature distribution inside cooling chamber is given in Fig. 19. This result obtained from CFD shows a good agreement with the thermal camera images in Fig. 13. As can be seen in the numerical results, the coldest parts are the aluminum bars and their surroundings and the base of the cooling chamber. The lowest temperature of 5 °C obtained in the contour corresponds strongly with the minimum temperature value taken from the thermal camera. A similar situation is also seen for the external heat exchanger given in Fig. 15. By validating the numerical results with experimental data, it is considered that CFD simulation results are given with a high confidence level.

#### 4. Conclusions and future work

The most important part of this work is assigned to the innovative design and production of the solar powered Peltier cooling system based on the natural convection mechanism without the need for extra tools (fan, pump etc.). In this study, an effective cooling performance was achieved by increasing the heat transfer surface area by adding aluminum bars to the lower exchanger at the cooling chamber and adding perforated aluminum sheets to the upper exchanger as a new

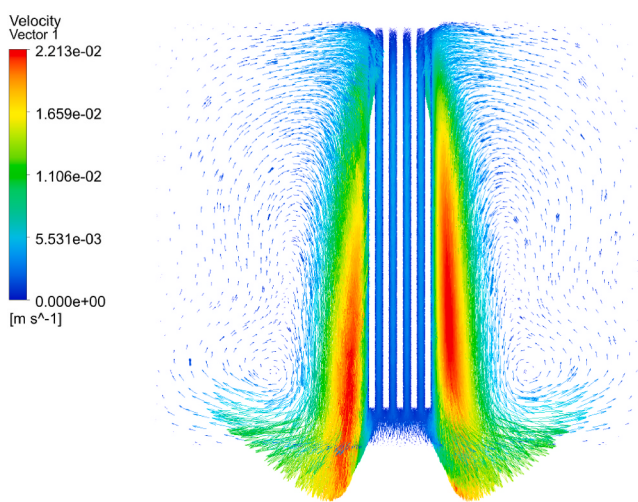
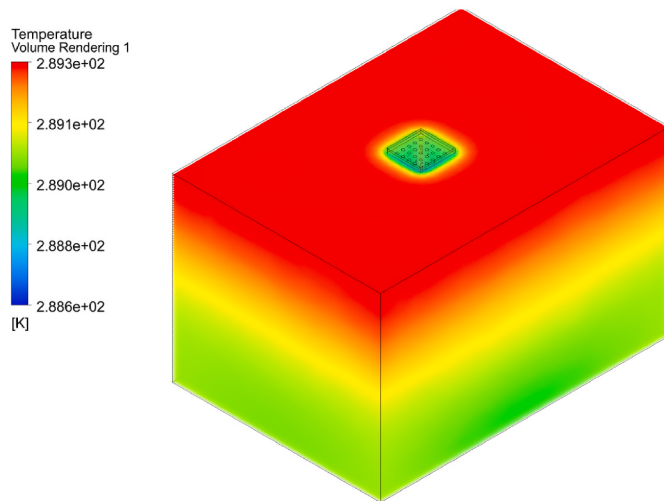
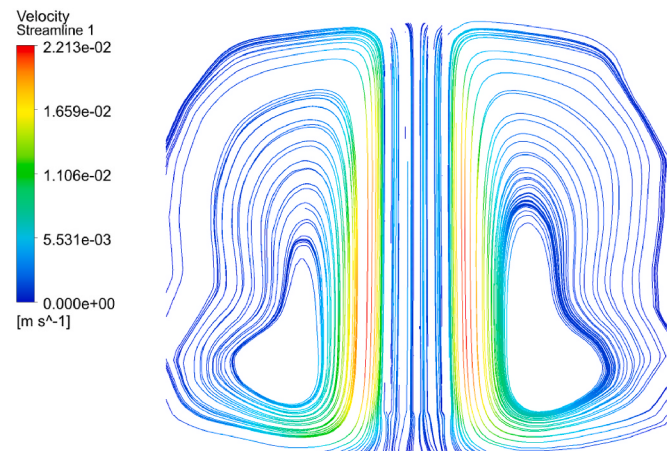
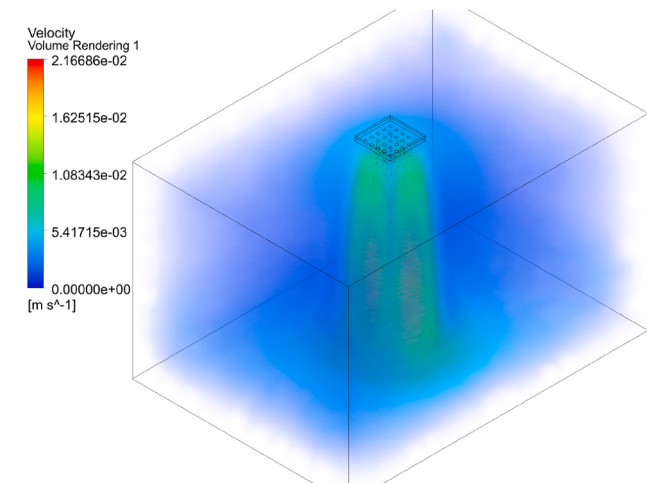


**Fig. 17.** Velocity and temperature volume rendering results of cooling chamber.

type of boosted heat exchanger. In this research, the number of Peltier modules was changed to 3 Peltier and 5 Peltier modes in order to optimize and increase the COP value and to compare with the single type Peltier system. Optimization study was also performed by applying different voltage values. The maximum COP value was obtained at 1.5 V as 0.04 for the single Peltier mode. The COP value decreased continuously over time under all operating conditions. Therefore, the average COP values were calculated and the highest value was calculated as 0.0103. Additionally, the minimum temperature value obtained inside the cooling chamber was 11.28 °C in 5 Peltiers mode and under 3 V voltage. CFD study was performed for all domains of cooling system and temperature distributions and air flow structure were evaluated. Although TE coolers have a low COP value, different studies can be carried out to improve the performance. Some of the scopes of future works related to this present work can be listed as, design of water-to-water TE home refrigerator, an investigation on the TE cooling performance under pulsed electrical loads, the use of different heat sink block sizes, the application of different methods (such as fluid cooled, air cooled) to remove waste heat from the cooling chamber, the effect of heat generation of the fans inside cooling box, and also Increasing the operating performance of the system by detecting and preventing heat losses.

**Fig. 18.** Streamlines and velocity vectors results of cooling chamber.

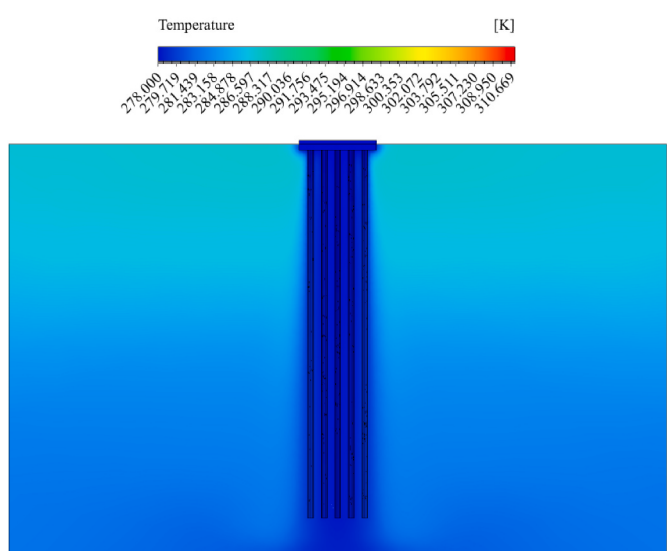


**Fig. 19.** Temperature distribution inside cooling chamber.

#### CRediT authorship contribution statement

**Faraz Afshari:** Methodology, Conceptualization, Software, Investigation. **Emre Mandev:** Investigation, Methodology, Writing – original

**draft. Burak Muratçobanoğlu:** Formal analysis, Software, Visualization. **Ali Fatih Yetim:** Formal analysis, Investigation. **Mehmet Akif Ceviz:** Visualization, Supervision.

## Declaration of competing interest

The authors declare that they have no known competing financial interests or personal relationships that could have appeared to influence the work reported in this paper.

## Acknowledgments

This project was supported by Research Project Foundation of the Erzurum Technical University (BAP Project No. 2020/10). The authors of this research gratefully acknowledge the support of this study.

## References

- [1] S.M. Pourkiaei, M.H. Ahmadi, M. Sadeghzadeh, S. Moosavi, F. Pourfayaz, L. Chen, R. Kumar, Thermoelectric cooler and thermoelectric generator devices: a review of present and potential applications, modeling and materials, *Energy* 186 (2019), 115849.
- [2] B. Ohara, R. Sitar, J. Soares, P. Novisoff, A. Nunez-Perez, H. Lee, Optimization strategies for a portable thermoelectric vaccine refrigeration system in developing communities, *J. Electron. Mater.* 44 (6) (2015) 1614–1626.
- [3] R.S. Srivastava, A. Kumar, H. Thakur, R. Vaish, Solar assisted thermoelectric cooling/heating system for vehicle cabin during parking: a numerical study, *Renew. Energy* 181 (2022) 384–403.
- [4] D. Luo, R. Wang, W. Yu, W. Zhou, Parametric study of a thermoelectric module used for both power generation and cooling, *Renew. Energy* 154 (2020) 542–552.
- [5] A. Zuazua-Ros, C. Martín-Gómez, E. Ibañez-Puy, M. Vidaurre-Arbizu, Y. Gelbstein, Investigation of the thermoelectric potential for heating, cooling and ventilation in buildings: characterization options and applications, *Renew. Energy* 131 (2019) 229–239.
- [6] A. Provensi, J.R. Barbosa Jr., Analysis and optimization of air coolers using multiple-stage thermoelectric modules arranged in counter-current flow, *Int. J. Refrig.* 110 (2020) 19–27.
- [7] X.X. Tian, S. Asaadi, H. Moria, A. Kaood, S. Pourhedayat, K. Jermsittiparsert, Proposing tube-bundle arrangement of tubular thermoelectric module as a novel air cooler, *Energy* 208 (2020), 118428.
- [8] M. Cosnier, G. Fraisse, L. Luo, An experimental and numerical study of a thermoelectric air-cooling and air-heating system, *Int. J. Refrig.* 31 (6) (2008) 1051–1062.
- [9] M. Ibañez-Puy, J. Bermejo-Busto, C. Martín-Gómez, M. Vidaurre-Arbizu, J. A. Sacristán-Fernández, Thermoelectric cooling heating unit performance under real conditions, *Appl. Energy* 200 (2017) 303–314.
- [10] H.S. Dizaji, S. Jafarmadar, S. Khalilarya, S. Pourhedayat, A comprehensive exergy analysis of a prototype Peltier air-cooler; experimental investigation, *Renew. Energy* 131 (2019) 308–317.
- [11] E. Yin, Q. Li, Achieving extensive lossless coupling of photovoltaic and thermoelectric devices through parallel connection, *Renew. Energy* 193 (2022) 565–575.
- [12] X. Su, L. Zhang, Z. Liu, Y. Luo, D. Chen, W. Li, Performance evaluation of a novel building envelope integrated with thermoelectric cooler and radiative sky cooler, *Renew. Energy* 171 (2021) 1061–1078.
- [13] K.K.I. Al-Chlaihawi, A. Al-Saadi, N.A. Jabbar, An experimental and theoretical study of forced convection from a peltier thermo-electric cooling, in: IOP Conference Series: Materials Science and Engineering 870, IOP Publishing, 2020, June, 012166. No. 1.
- [14] A. Winarta, I.M. Rasta, L.P.I. Midiani, I.W.A. Subagia, A.A.N.G. Sapteka, Experimental study of thermoelectric cooler box using heat sink with u-shape heat pipe and methanol working fluid, *IOP Conf. Ser. Mater. Sci. Eng.* 1034 (1) (2021, February), 012033.
- [15] J.G. Vian, D. Astrain, Development of a heat exchanger for the cold side of a thermoelectric module, *Appl. Therm. Eng.* 28 (11–12) (2008) 1514–1521.
- [16] G. Min, D.M. Rowe, Experimental evaluation of prototype thermoelectric domestic-refrigerators, *Appl. Energy* 83 (2) (2006) 133–152.
- [17] A. Çağlar, Optimization of operational conditions for a thermoelectric refrigerator and its performance analysis at optimum conditions, *Int. J. Refrig.* 96 (2018) 70–77.
- [18] A. Martínez, D. Astrain, A. Rodríguez, G. Pérez, Reduction in the electric power consumption of a thermoelectric refrigerator by experimental optimization of the temperature controller, *J. Electron. Mater.* 42 (7) (2013) 1499–1503.
- [19] H.S. Huang, Y.C. Weng, Y.W. Chang, S.L. Chen, M.T. Ke, Thermoelectric water-cooling device applied to electronic equipment, *Int. Commun. Heat Mass Tran.* 37 (2) (2010) 140–146.
- [20] M. Gökcük, F. Şahin, Experimental performance investigation of minichannel water cooled-thermoelectric refrigerator, *Case Stud. Therm. Eng.* 10 (2017) 54–62.
- [21] E. Söylemez, E. Alpman, A. Onat, Experimental analysis of hybrid household refrigerators including thermoelectric and vapour compression cooling systems, *Int. J. Refrig.* 95 (2018) 93–107.
- [22] Y.W. Gao, H. Lv, X.D. Wang, W.M. Yan, Enhanced Peltier cooling of two-stage thermoelectric cooler via pulse currents, *Int. J. Heat Mass Tran.* 114 (2017) 656–663.
- [23] C.J. Hermes, J.R. Barbosa Jr., Thermodynamic comparison of Peltier, Stirling, and vapor compression portable coolers, *Appl. Energy* 91 (1) (2012) 51–58.
- [24] J.S. Lee, S.H. Rhi, C.N. Kim, Y. Lee, Use of two-phase loop thermosyphons for thermoelectric refrigeration: experiment and analysis, *Appl. Therm. Eng.* 23 (9) (2003) 1167–1176.
- [25] H. Yadav, D. Srivastav, G. Kumar, A.K. Yadav, A. Goswami, Experimental investigations and analysis of thermoelectric refrigerator with multiple peltier modules, *Int. J. Trend Scientific Res. Develop.* 3 (2019) 1337–1340.
- [26] D. Astrain, J.G. Vián, J. Albizu, Computational model for refrigerators based on Peltier effect application, *Appl. Therm. Eng.* 25 (17–18) (2005) 3149–3162.
- [27] S.B. Riffat, X. Ma, Improving the coefficient of performance of thermoelectric cooling systems: a review, *Int. J. Energy Res.* 28 (9) (2004) 753–768.
- [28] A. Martínez, D. Astrain, A. Rodriguez, P. Aranguren, Advanced computational model for Peltier effect based refrigerators, *Appl. Therm. Eng.* 95 (2016) 339–347.
- [29] K. Posobkiewicz, K. Górecki, Influence of selected factors on parameters of a cooling system with a Peltier module and forced air flow, *Microelectron. Int.* (2021) 1–6.
- [30] M. Baldry, V. Timchenko, C. Menictas, Optimal design of a natural convection heat sink for small thermoelectric cooling modules, *Appl. Therm. Eng.* 160 (2019), 114062.
- [31] M. Awasthi, K.V. Mali, Design and development of thermoelectric refrigerator, *Int. J. Mech. Eng. Robotic. Res.* 1 (3) (2012) 5418–5421.
- [32] Y. He, R. Li, Y. Fan, Y. Zheng, G. Chen, Study on the performance of a solid-state thermoelectric refrigeration system equipped with ionic wind fans for ultra-quiet operation, *Int. J. Refrig.* 130 (2021) 441–451.
- [33] S. Jugsujinda, A. Vora-ud, T. Seetawan, Analyzing of thermoelectric refrigerator performance, *Procedia Eng.* 8 (2011) 154–159.
- [34] S.M.A. Rahman, A.A. Hachicha, C. Ghenai, R. Saidur, Z. Said, Performance and life cycle analysis of a novel portable solar thermoelectric refrigerator, *Case Stud. Therm. Eng.* 19 (2020), 100599.
- [35] A.D. Tuncer, A. Sözen, A. Khanlari, A. Amini, C. Şirin, Thermal performance analysis of a quadruple-pass solar air collector assisted pilot-scale greenhouse dryer, *Sol. Energy* 203 (2020) 304–316.
- [36] E. Çiftçi, A. Khanlari, A. Sözen, İ. Aytaç, A.D. Tuncer, Energy and exergy analysis of a photovoltaic thermal (PVT) system used in solar dryer: a numerical and experimental investigation, *Renew. Energy* 180 (2021) 410–423.
- [37] A.D. Tuncer, A. Sözen, A. Khanlari, E.Y. Gürbüz, H.I. Variyenli, Analysis of thermal performance of an improved shell and helically coiled heat exchanger, *Appl. Therm. Eng.* 184 (2021), 116272.
- [38] Y.W. Chang, C.C. Chang, M.T. Ke, S.L. Chen, Thermoelectric air-cooling module for electronic devices, *Appl. Therm. Eng.* 29 (13) (2009) 2731–2737.
- [39] F. Afshari, Experimental and numerical investigation on thermoelectric coolers for comparing air-to-water to air-to-air refrigerators, *J. Therm. Anal. Calorimetry* 144 (3) (2021) 855–868.
- [40] I.B. Tijani, A.A. Al Hamadi, K.A. Al Naqbi, R.I. Almarzoqi, N.K. Al Rahbi, Development of an automatic solar-powered domestic water cooling system with multi-stage Peltier devices, *Renew. Energy* 128 (2018) 416–431.
- [41] A. Sözen, C. Şirin, A. Khanlari, A.D. Tuncer, E.Y. Gürbüz, Thermal performance enhancement of tube-type alternative indirect solar dryer with iron mesh modification, *Sol. Energy* 207 (2020) 1269–1281.
- [42] F. Afshari, Experimental and numerical study on using forced convection to increase heat transfer in home radiators by employing solar cells and fans, *Heat Tran. Res.* 51 (1) (2020) 1–12.
- [43] L. Pan, H. Wang, Q. Chen, C. Chen, Theoretical and experimental study on several refrigerants of moderately high temperature heat pump, *Appl. Therm. Eng.* 31 (11–12) (2011) 1886–1893.
- [44] R.R. He, H.Y. Zhong, Y. Cai, D. Liu, F.Y. Zhao, Theoretical and experimental investigations of thermoelectric refrigeration box used for medical service, *Procedia Eng.* 205 (2017) 1215–1222.
- [45] S.A. Abdul-Wahab, A. Elkamel, A.M. Al-Damkhi, A. Is' Haq, H.S. Al-Rubai'ey, A. K. Al-Battashi, A.R. Al-Tamimi, K.H. Al-Mamari, M.U. Chutani, Design and experimental investigation of portable solar thermoelectric refrigerator, *Renew. Energy* 34 (1) (2009) 30–34.
- [46] M.A. Rahman, C.Y. Sianipar, A.I. Majid, A. Widyatama, Suhanan, Experimental study of the effects of input voltage on the transient temperature behaviors of thermoelectric mini-cold storage, in: AIP Conference Proceedings 2248, AIP Publishing LLC, 2020, 070003. No. 1.
- [47] V.K. Dongare, R.V. Kinare, M.H. Parkar, R.P. Salunke, Design and development of thermoelectric refrigerator, *Int. Res. J. Eng. Technol.* 5 (4) (2018).
- [48] F. Afshari, M.A. Ceviz, E. Mandev, F. Yıldız, Effect of heat exchanger base thickness and cooling fan on cooling performance of Air-To-Air thermoelectric refrigerator; experimental and numerical study, *Sustain. Energy Technol. Assessments* 52 (2022), 102178.
- [49] J. Luo, L. Chen, F. Sun, C. Wu, Optimum allocation of heat transfer surface area for cooling load and COP optimization of a thermoelectric refrigerator, *Energy Convers. Manag.* 44 (20) (2003) 3197–3206.
- [50] M. Mirmanto, S. Syahrul, Y. Wirdan, Experimental performances of a thermoelectric cooler box with thermoelectric position variations, *Eng. Sci. Technol. Int. J.* 22 (1) (2019) 177–184.
- [51] M. Siahmargoi, N. Rahbar, H. Kargarsharifabad, S.E. Sadati, A. Asadi, An experimental study on the performance evaluation and thermodynamic modeling of a thermoelectric cooler combined with two heatsinks, *Sci. Rep.* 9 (1) (2019) 1–11.

- [52] M.A. Ceviz, F. Afshari, B. Muratçobanoğlu, M. Ceylan, E. Manay, Computational fluid dynamics simulation and experimental investigation of a thermoelectric system for predicting influence of applied voltage and cooling water on cooling performance, *Int. J. Numer. Methods Heat Fluid Flow* 33 (1) (2022) 241–262.
- [53] A.E. Gürel, Ü. Ağbulut, A. Ergün, İ. Ceylan, A. Sözen, A.D. Tuncer, A. Khanlari, A detailed investigation of the temperature-controlled fluidized bed solar dryer: a numerical, experimental, and modeling study, *Sustain. Energy Technol. Assessments* 49 (2022), 101703.
- [54] A. Khanlari, A. Sözen, F. Afshari, A.D. Tuncer, Ü. Ağbulut, Z.A. Yılmaz, Numerical and experimental analysis of parallel-pass forced convection solar air heating wall with different plenum and absorber configurations, *Int. J. Numer. Methods Heat Fluid Flow* (2021).
- [55] F. Afshari, A.D. Tuncer, A. Sözen, E. Çiftçi, A. Khanlari, Experimental and numerical analysis of a compact indirect solar dehumidification system, *Sol. Energy* 226 (2021) 72–84.